Brain Pathology ISSN 1015-6305

RESEARCH ARTICLE

Altered Adhesive Structures and Their Relation to RhoGTPase Activation in Merlin-Deficient Schwannoma

Christine Flaiz[1]; Sylwia Ammoun, PhD[1]; Anja Biebl, MD[2]; C. Oliver Hanemann, MD, PhD[1]

[1] Department of Clinical Neurobiology, Institute of Biomedical and Clinical Science, Peninsula College for Medicine and Dentistry, Plymouth PL6 8BU, UK.

[2] Department of Neurology, Zentrum fuer Klinische Forschung, University of Ulm, Ulm 89069, Germany.

Keywords
merlin, GTPases, schwannoma, focal contacts, adhesion, neurofibromatosis.

Corresponding author:
C. Oliver Hanemann, MD, PhD, Clinical Neurobiology, Peninsula College for Medicine and Dentistry, The John Bull Building, Tamar Science Park, Research Way, Plymouth PL6 8BU, UK (E-mail: *oliver.hanemann@pms.ac.uk*)

Received 1 November 2007; accepted 5 February 2008.

doi:10.1111/j.1750-3639.2008.00165.x

Abstract

Schwannomas are Schwann cell tumors of the nervous system that occur spontaneously and in patients with neurofibromatosis 2 (NF2) and lack the tumor suppressor merlin. Merlin is known to bind paxillin, beta1 integrin and focal adhesion kinase, members of focal contacts, multi-protein complexes that mediate cell adhesion to the extracellular matrix. Moreover, merlin-deficient Schwannomas show pathological adhesion to the extracellular matrix making the characterization of focal contacts indispensable. Using our Schwannoma *in vitro* model of human primary Schwann and Schwannoma cells, we here show that Schwannoma cells display an increased number of mature and stable focal contacts. In addition to an involvement of RhoA signaling via the Rho kinase ROCK, Rac1 plays a significant role in the pathological adhesion of Schwannoma cells. The Rac1 guanine exchange factor—beta-Pix, localizes to focal contacts in human primary Schwannoma cells, and we show that part of the Rac1 activation, an effect of merlin-deficiency, occurs at the level of focal contacts in human primary Schwannoma cells. Our results help explaining the pathological adhesion of Schwannoma cells, further strengthen the importance of RhoGTPase signaling in Schwannoma development, and suggest that merlin's role in tumor suppression is linked to focal contacts.

INTRODUCTION

Loss of the tumor suppressor protein merlin [neurofibromatosis 2 (NF2)] accounts for human Schwannomas that occur spontaneously or in patients with the inherited cancer predisposition disease NF2. Schwann cells are peripheral glia cells that insert cytoplasmic extensions into bundles of axons to sort, ensheath and myelinate them (19). Signals from the extracellular matrix are important for axonal sorting, and therefore, myelination, a process that is highly regulated by RhoGTPases (2, 21, 31, 43). Schwannomas are benign Schwann cell tumors (14) that show increased adhesion to the extracellular matrix because of the activation of integrins alpha6, beta1 and beta4 (46), and instead of myelinating an axon, Schwannoma cells rather ensheath the extracellular matrix, resulting in so-called pseudomesaxons (9). Loss of merlin in Schwannomas has been linked to many cellular protrusions (11, 35), loss of cell-cell-adhesion (12, 23) and increased cell spreading (37, 47). Merlin has a broad tumor suppressor function (27, 40, 44), but as it lacks any DNA-binding or catalytic domain, it seems that merlin is a rather unusual tumor suppressor (33). Focal contacts are large multi-protein complexes that mediate adhesion of the cell to the extracellular matrix (3, 4, 53). They are highly dynamic and can be subdivided into the small, short-living and mostly lamellipodia-associated focal complexes and the more mature, large and stable focal adhesions (51). Whereas, both structures contain paxillin and the focal adhesion kinase (FAK) (16, 30), only focal complexes interact with the Arp2/3 complex which is important in actin-branching, and therefore, in the formation of protrusion (8). Focal adhesions lack the Arp2/3 complex, but embody zyxin and can be found more distant from the lamellipodium, at the tips of actin stress fibers. The hypothesis that merlin exerts its tumor suppressor function partially at the level of focal contacts is tempting, especially as it binds beta1 integrin in Schwann cells (32), paxillin (10) and FAK (17). Moreover, merlin inhibits the p21-activated kinase PAK and thereby suppresses Rac1 activation that is a prominent characteristic of merlin-deficient Schwannoma (15, 20, 22, 49). Interestingly, the p21-activated kinase PAK localizes to focal contacts in a complex with Pix, a guanine exchange factor (GEF) which activates Rac1 (38, 54). Focal contacts are themselves regulated by RhoGTPases (36) and Rac1 that is activated in Schwannomas (20, 35), and has been implicated in the regulation of focal complexes (21).

Knowledge about focal contacts, their characteristics and regulation in Schwannoma could, therefore, promote an insight into why Schwannoma show pathological adhesion and form pseudomesaxons, and contribute to the understanding of how merlin exerts its tumor suppressor function.

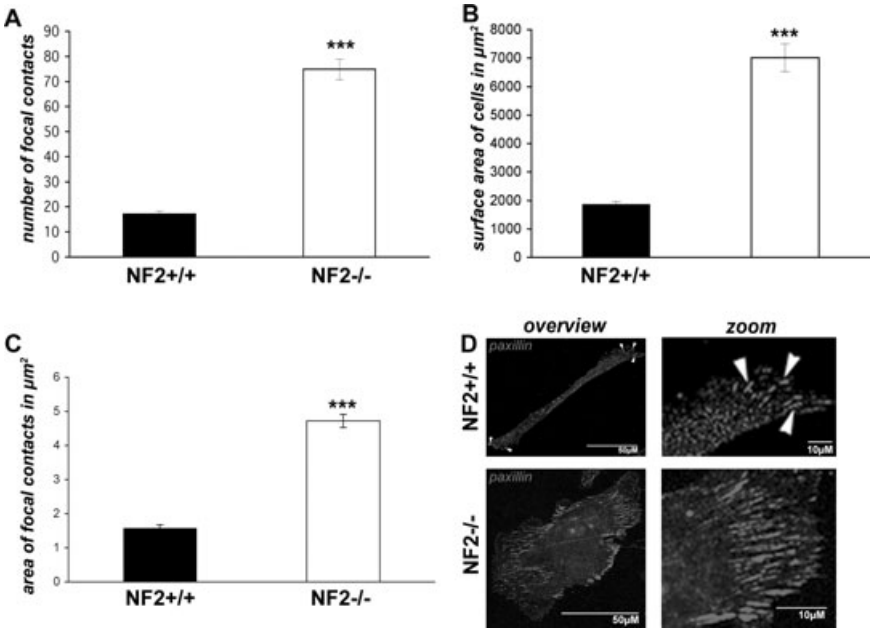

Figure 1. *Number and size of focal contacts in human primary Schwann (NF2+/+) and Schwannoma cells (NF2–/–).* **A.** Paxillin staining reveals that human primary Schwann cells (NF2+/+) exhibit only 17 ± 1 focal contacts, whereas human primary Schwannoma cells (NF2–/–) contain on average 75 ± 4 focal contacts (***: very highly significant; $P < 0.001$ in student's *t*-test). **B.** The surface area of human primary Schwann cells (NF2+/+) is on average 1869.7 ± 98.2 µm² and of human primary Schwannoma cells (NF2–/–) 7019.8 ± 497.2 µm² (***: very highly significant; $P < 0.001$ in student's *t*-test). The larger surface area in Schwannoma cells corresponds with the number of focal contacts. **C.** Focal contacts that have been identified through the representative marker paxillin, show an average size of 1.6 ± 0.1 µm² in Schwann cells (NF2+/+). Schwannoma cells (NF2–/–) show markedly bigger focal contacts with an average size of 4.7 ± 0.2 µm² (***: very highly significant; $P < 0.001$ in student's *t*-test). **D.** Example of paxillin-stained human primary Schwann (NF2+/+) and Schwannoma cells (NF2–/–) showing only few, small and lamellipodia-associated focal contacts in Schwann cells and numerous, big and ubiquitously distributed focal contacts in Schwannoma cells. NF = neurofibromatosis.

Using our Schwannoma *in vitro* model of healthy human primary Schwann and human primary Schwannoma cells, we here show that focal contacts in human Schwannoma cells differ markedly in number, size, molecular composition and turnover dynamics from their counterparts in healthy human primary Schwann cells. We show that the RhoGTPases RhoA and Rac1 are involved in these alterations of adhesion in Schwannomas. Moreover, the increased Rac1 activation seems to occur at least partly through the focal contact associated GEF beta-Pix. Thus, we suggest that merlin exerts its tumor suppressor function to some extent at levels of focal contacts.

RESULTS

Characterization of focal contacts

Merlin-deficient human primary Schwannoma cells show increased adhesion to the extracellular matrix (46). As adhesion is mediated by focal contacts, large multi-protein complexes that link the cytoskeleton of the cell to the extracellular matrix, we initially investigated adhesive structures in Schwannoma cells. We first determined number of focal contacts in human primary Schwann and Schwannoma cells that have been stained for the representative focal contact marker paxillin. Whereas, an average human primary Schwann cell showed only about 17 ± 1 focal contacts, Schwannoma cells displayed around 75 ± 4 focal contacts per cell (Figure 1A). According to the increase in focal contacts, human primary Schwannoma cells were more spread on laminin and exhibited a larger surface area (around 7019 ± 497.2 µm² compared with 1869.7 ± 98.24 µm² in Schwann cells) (Figure 1B). Figure 1C shows that focal contacts were much bigger in human primary Schwannoma cells (4.7 ± 0.2 µm² compared with 1.6 ± 0.1 µm² in human primary Schwann cells). The differences in number and size of focal contacts between Schwann and Schwannoma cells are very highly significant ($P < 0.001$ in student's *t*-test). The data indicate that Schwannoma cells have more and bigger focal contacts compared with Schwann cells. This can also be seen in the exemplified overview and zoomed images of paxillin-stained human primary Schwann and Schwannoma cells (Figure 1D). Very similar results were obtained when cells were stained for FAK or the autophosphorylated, and therefore, activated form of FAK, phospho-FAK Y397 (data not shown).

The marked differences in number and size between Schwann and Schwannoma cells could point to different maturity states of focal contacts. Focal contacts can be sub-grouped into focal complexes and focal adhesions (51, 52). Focal complexes are short-living and small, and can be found in the lamellipodia in association with the Arp2/3 complex. When focal complexes mature they get bigger and more stable because of the incorporation of further proteins like zyxin and the association with actin stress fibers. We

thus performed co-localization studies of paxillin present in both, focal complexes and focal adhesions, with the Arp2/3 complex subunit p34-Arc, zyxin and F-actin. Focal contacts in Schwann cells could be found in the lamellipodia in close proximity to the Arp2/3 complex (arrows), as co-localization of paxillin with p34-Arc shows (Figure 2A, see inset for higher magnification). In Schwannoma cells, however, no co-localization of paxillin with p34-Arc could be detected (Figure 2B). In accordance to these findings no zyxin, a marker of the mature focal adhesions could be found in focal contacts in Schwann cells (Figure 2C); however, Schwannoma cells showed a strong co-localization of paxillin with zyxin (Figure 2D). Moreover, most focal contacts in human primary Schwann cells were dispersed throughout the lamellipodium (Figure 2E). Focal contacts in Schwannoma cells mostly localize to the tips of actin stress fibers (Figure 2F). Taken together, focal contacts in Schwann cells are mainly short-living and lamellipodia-associated focal complexes, whereas Schwannoma cells exhibit mainly mature focal adhesions. As an additional control, we reintroduced merlin into human primary Schwannoma cells, using an adenovirus. After infection of Schwannoma cells with merlin (NF2)-Green fluorescent protein (GFP) adenoviral supernatant, about 90% of all cells showed expression of merlin at variable levels. GFP-expressing cells also express merlin, as has been confirmed by immunocytochemical staining, using a merlin primary antibody (data not shown). Uninfected and GFP-infected human primary Schwannoma cells show many, big and ubiquitously distributed focal contacts, that do not co-localize with the p34-Arc subunit of the Arp2/3 complex (Figure 3A,B). Forty-eight hours after merlin reintroduction, when merlin expression is best, merlin re-expressing human primary Schwannoma cells exhibit an elongated morphology like healthy Schwann cells with nearly no focal contacts in the lamellipodium. Paxillin staining, however, can be found in close proximity to the Arp2/3 complex subunit p34-Arc (Figure 3C).

Dynamics of focal contacts

Focal contacts are normally regulated by quick assembly and disassembly (51). The increased number, size and maturity of focal contacts in Schwannoma cells point to a disturbance in the disassembly of those structures. To investigate turnover of focal contacts live cell imaging of paxillin-GFP and zyxin-GFP transfected human primary Schwann, and Schwannoma cells was performed. Focal contacts were observed for 24 minutes (within that time span turnover of focal contacts has been observed in Schwann cells) and changes in size and intensity were measured. According to the change three different categories of focal contacts were defined: Focal contacts that were smaller and less intense or completely disappeared during the observed time span were classified as "disappeared and smaller". If no change in size and intensity could be observed, focal contacts were classified as "equal". Focal contacts that could be detected only at the end of the observed time span or were bigger and more intense were classified as "appeared and bigger". Whereas Schwann and Schwannoma cells showed an equal number of focal contacts in the category 3 "appeared and bigger" (non-significant difference in student's *t*-test), indicating that both have the same assembly rate of focal contacts, Schwannoma cells showed fewer focal contacts that disassemble or get smaller compared with Schwann cells (Figure 4A) ($P < 0.05$ in students *t*-test). In line with that Schwannoma cells displayed more focal contacts that didn't change size and intensity (category "equal") than Schwann cells ($P < 0.05$ in student's *t*-test). Both constructs give comparable patterns for the turnover rate in our system. The alterations in turnover of focal contacts in Schwann vs. Schwannoma cells were further investigated by color-coding the obtained images. The initial images (time-point 1; 0 minutes) were colored in green and the last images (time-point 2; 24 minutes) were colored red. When both pictures were overlaid only stable focal contacts would appear in yellow. Figure 4B shows representative zyxin-GFP transfected cells. Focal contacts in Schwann cells changed their position and shape when the image from time-point 1 is compared with that at time-point 2 and accordingly nearly no overlap in yellow could be observed. In Schwannoma cells, most of the focal contacts did not change their position or their shape and in line with that they appeared clearly yellow in the overlay image. Comparable results were obtained when using paxillin-GFP transfected cells. Taken together these findings suggest that focal contacts in human primary Schwannoma cells are more stable because of impaired disassembly. Figure 4C shows endogenous zyxin expression in human primary Schwann and Schwannoma cells and zyxin-GFP after transfection. The transfection process does not lead to changes in the morphology of neither Schwann nor Schwannoma cells. This is also true for the transfection with paxillin (data not shown).

Regulation of adhesion and focal contacts in human primary Schwannoma cells by RhoGTPases

RhoGTPases are involved in cellular processes like protrusion, migration and also adhesion (13). The RhoGTPase RhoA is supposed to regulate stress fibers and the formation and turnover of focal adhesions (5). Pelton *et al* (35) have previously shown that Schwannoma cells lost stress fibers and focal adhesions when RhoA was blocked with C3 transferase, which catalyzes ADP ribosylation or when using a dominant-negative construct, and they suggested enhanced RhoA activity in Schwannoma. Using the GLISA method, we here show that Schwannoma cells did indeed exhibit significantly elevated levels of RhoA-GTP (Figure 5A) ($P < 0.05$ in student's *t*-test). Interestingly it has been shown that the RhoA kinase ROCKII is important for myelination of Schwann cells (28). We here blocked ROCK with the chemical inhibitor Y27632 (45) and stained cells with paxillin and Alexa Fluor 488-labeled phalloidin to visualize focal contacts and F-actin, respectively. Untreated Schwannoma cells exhibited many actin stress fibers with big focal adhesions at the tips of them (Figure 5B). Schwannoma cells treated with Y27632 lost stress fibres and paxillin-stained focal adhesions in a dose-dependent manner, pointing to a role of RhoA signaling through ROCK toward focal adhesions in Schwannomas. In concordance with the effects on focal contacts, 10 μM Y27632 reduced adhesion slightly to 78.20% of adhesion without inhibitor ($P < 0.05$ in student's *t*-test), and 20 μM Y27632 reduced adhesion to 60.10% ($P < 0.01$ in student's *t*-test) (Figure 5C).

Taken together, blocking of RhoA signaling through ROCK reduces number and size of focal adhesion and adhesion in a dose-dependent manner in human Schwannoma cells.

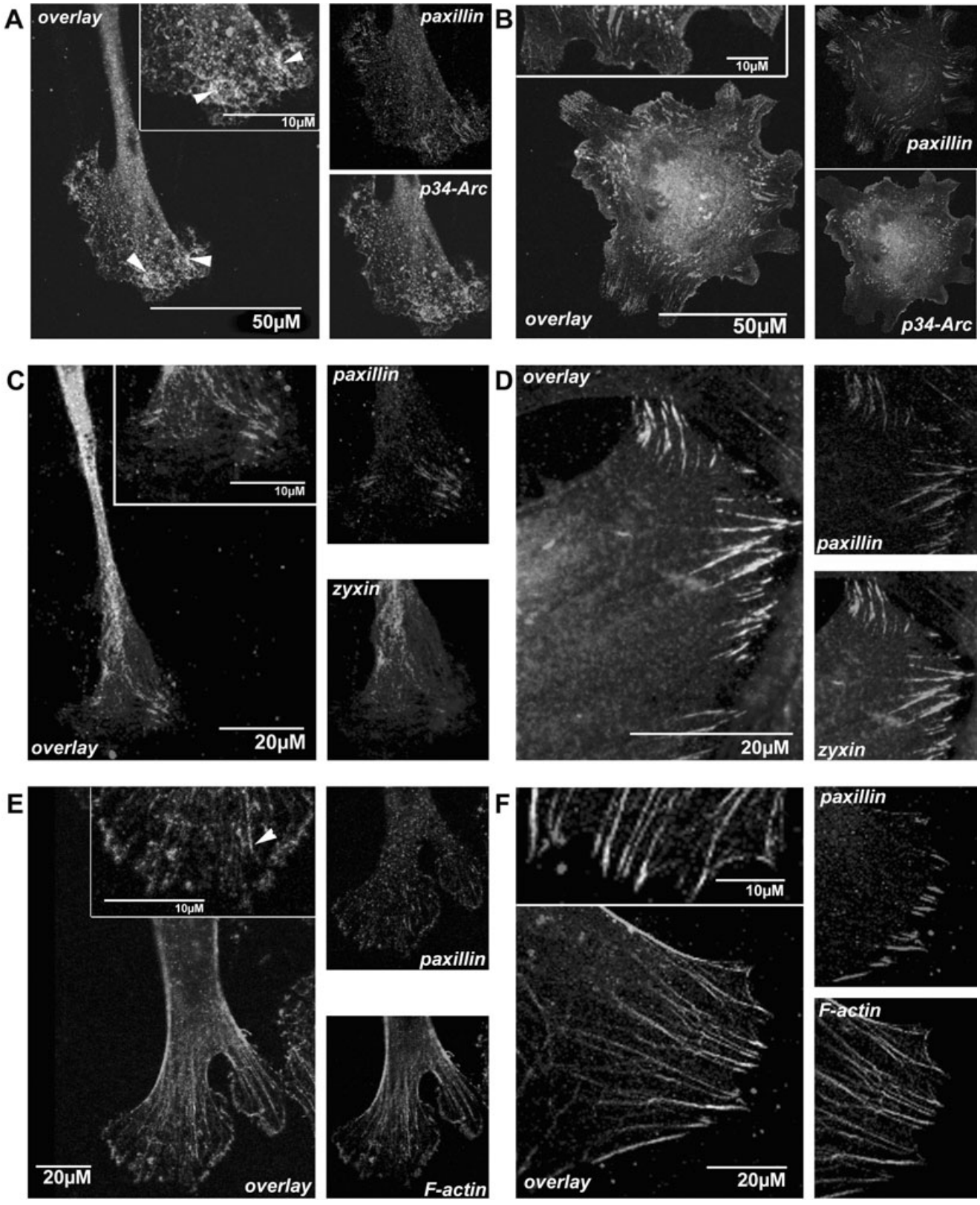

Figure 2. *Molecular characterization of focal contacts in human primary Schwann (NF2+/+) and Schwannoma cells (NF2–/–).* Paxillin staining found in focal contacts, i.e. short-living focal complexes as well as mature focal adhesions, is seen in close proximity with the Arp2/3 complex (see arrowheads) only in human primary Schwann cells (NF2+/+) (**A**), but not in human primary Schwannoma cells (NF2–/–) (**B**). In turn, focal contacts in human primary Schwann cells (NF2+/+) only rarely incorporate the focal adhesion marker zyxin (**C**), whereas focal contacts in human primary Schwannoma cells (NF2–/–) strongly stain for zyxin (**D**). Only few of the small focal contacts in human primary Schwann cells (NF2+/+) localize to the tip of stress fibers (arrowhead; F-actin has been stained using AlexaFluor 488 labeled phalloidin) (**E**). In human primary Schwannoma cells (NF2–/–) focal contacts can be found at the tip of stress fibers (**F**). NF = neurofibromatosis.

As merlin-deficient Schwannoma cells show elevated Rac1 activation (20), we wanted to know, if in addition to RhoA, Rac1 is involved in regulating adhesion in Schwannoma. Beta-Pix is a Rac1 GEF that is important for integrin-mediated Rac1 activation (7), and in a complex with PAK, co-localizes with paxillin in focal contacts (38). We, therefore, first analyzed beta-Pix localization in human primary Schwannoma cells. Immunocytochemical staining revealed that beta-Pix seems to localize to focal adhesions as it could be found in co-localization with paxillin (Figure 6A). ten Klooster *et al* (42) provided a model in which integrins and

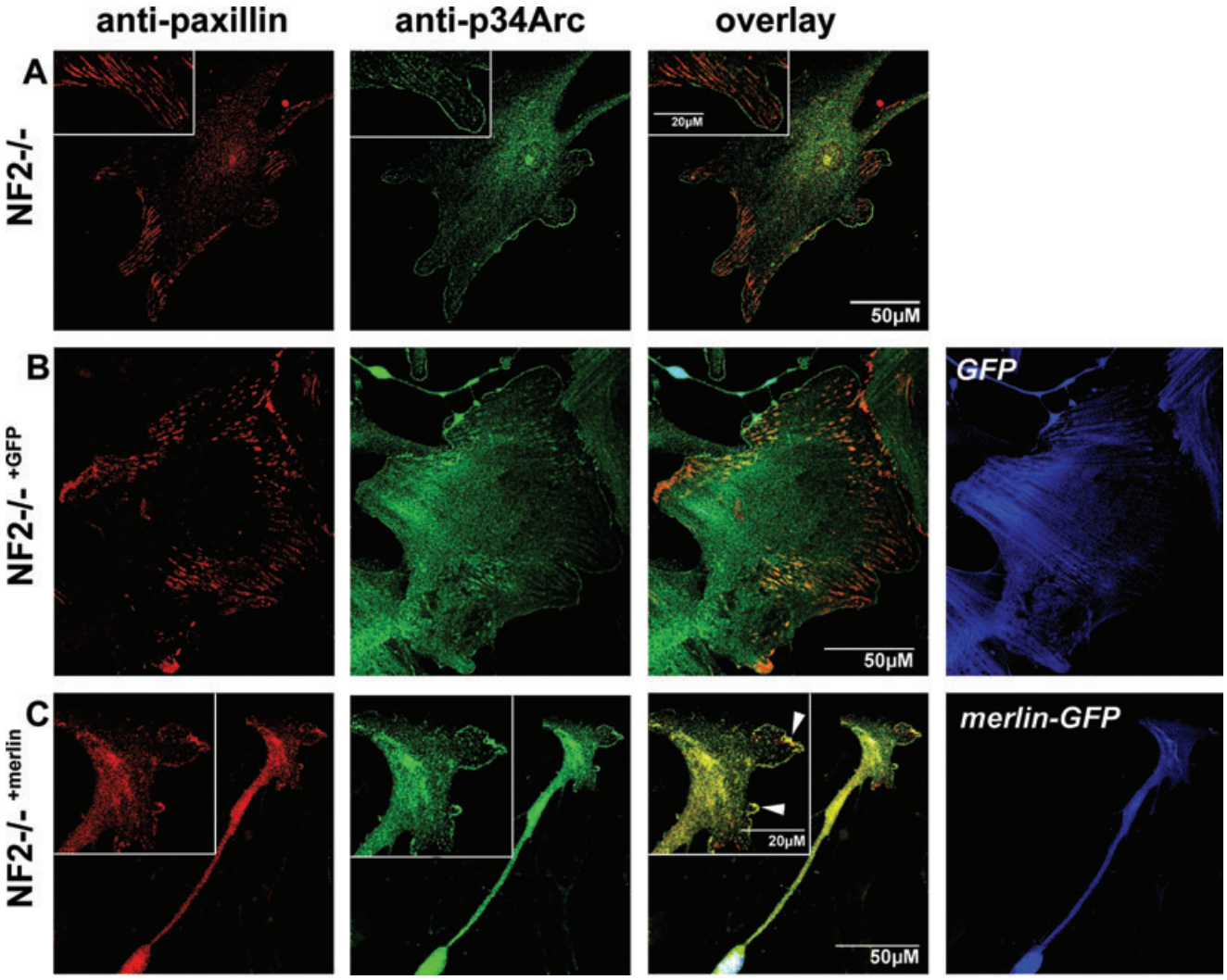

Figure 3. *Molecular characterization of focal contacts in merlin re-expressing human primary Schwannoma cells NF2–/–$^{+merlin}$.* **A.** The numerous large focal contacts that have been stained with paxillin, do not co-localize with the p34-Arc-subunit of the Arp2/3 complex in uninfected merlin-deficient human primary Schwannoma cells (NF2–/–). **B.** Infection with a control vector containing GFP alone does not alter the pattern of uninfected human primary Schwannoma cells: there is no co-localization between paxillin-stained focal contacts and the Arp2/3 complex. **C.** Merlin re-expressing human primary Schwannoma cells (NF2–/–$^{+merlin}$) show nearly no focal contacts and paxillin staining can be found around the membrane in the lamellipodium. Paxillin here strongly co-localizes with the Arp2/3 subunit p34-Arc (see arrowheads). NF = neurofibromatosis; GFP = green fluorescent protein.

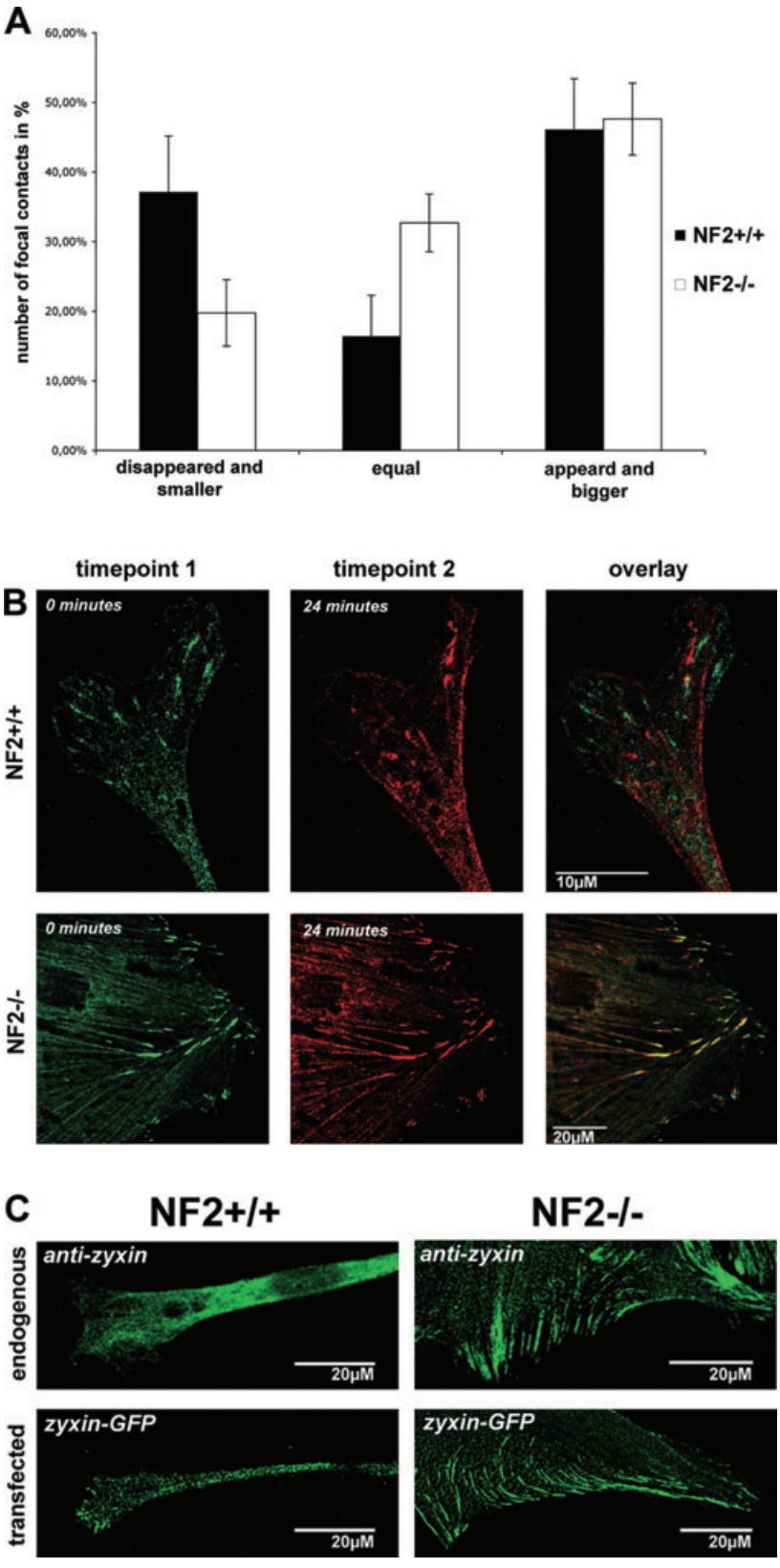

Figure 4. *Dynamics of focal contacts in paxillin-GFP and zyxin-GFP transfected human primary Schwann (NF2+/+) and Schwannoma cells (NF2–/–).* **A.** Cells have been investigated for 24 minutes using the Zeiss 510meta confocal microscope (63*). Focal contacts have been classified in one of three groups according to their total change in size and intensity over a period of 24 minutes. "Disappeared and smaller" for focal contacts that could not be detected after 24 minutes or had a negative total change in size and intensity, "equal" for focal contacts that did not change in size and intensity and "appeared and bigger" for focal contacts that could only be detected after 24 minutes or had a positive total change in size in intensity. 37.14% of the focal contacts in human primary Schwann cells (NF2+/+) disappeared or got smaller within 24 minutes; however, only 19.76% of focal contacts in human primary Schwannoma cells (NF2–/–) were classified in this group. In turn, only 16.41% of focal contacts where stable in Schwann cells (NF2+/+) compared with the 32.7% in Schwannoma cells (NF2–/–). The amount of focal contacts that appeared or grew bigger was similar in Schwann (NF2+/+) with 46.13% and Schwannoma cells (NF2–/–) with 47.61%. Changes in the categories "disappeared and smaller" and "equal" were significant (significant; $P < 0.05$ in student's *t*-test). **B.** To further illustrate focal contact turnover, images were color-coded (initial image: 0 minutes; green and last image: 24 minutes; red) and overlaid. The figure here illustrates a zyxin-GFP transfected Schwann (NF2+/+) and a zyxin-GFP transfected Schwannoma cell (NF2–/–). Focal contacts in Schwann cells (NF2+/+) change their shape and position and appear/disappear within the 24 minutes and nearly no overlay can be detected. In human primary Schwannoma cells (NF2–/–), however, most of the big focal contacts do not change size and position and appear yellow in the overlay image. Paxillin-GFP-transfected cells give the same pattern. **C.** Endogenous expression of zyxin and zyxin-GFP after transfection in human primary Schwann (NF2+/+) and Schwannoma cells (NF2–/–) prior to filming (time-point 0 minutes). Transfection with zyxin or paxillin (data not shown) does not alter the morphology of cells. NF = neurofibromatosis; GFP = green fluorescent protein.

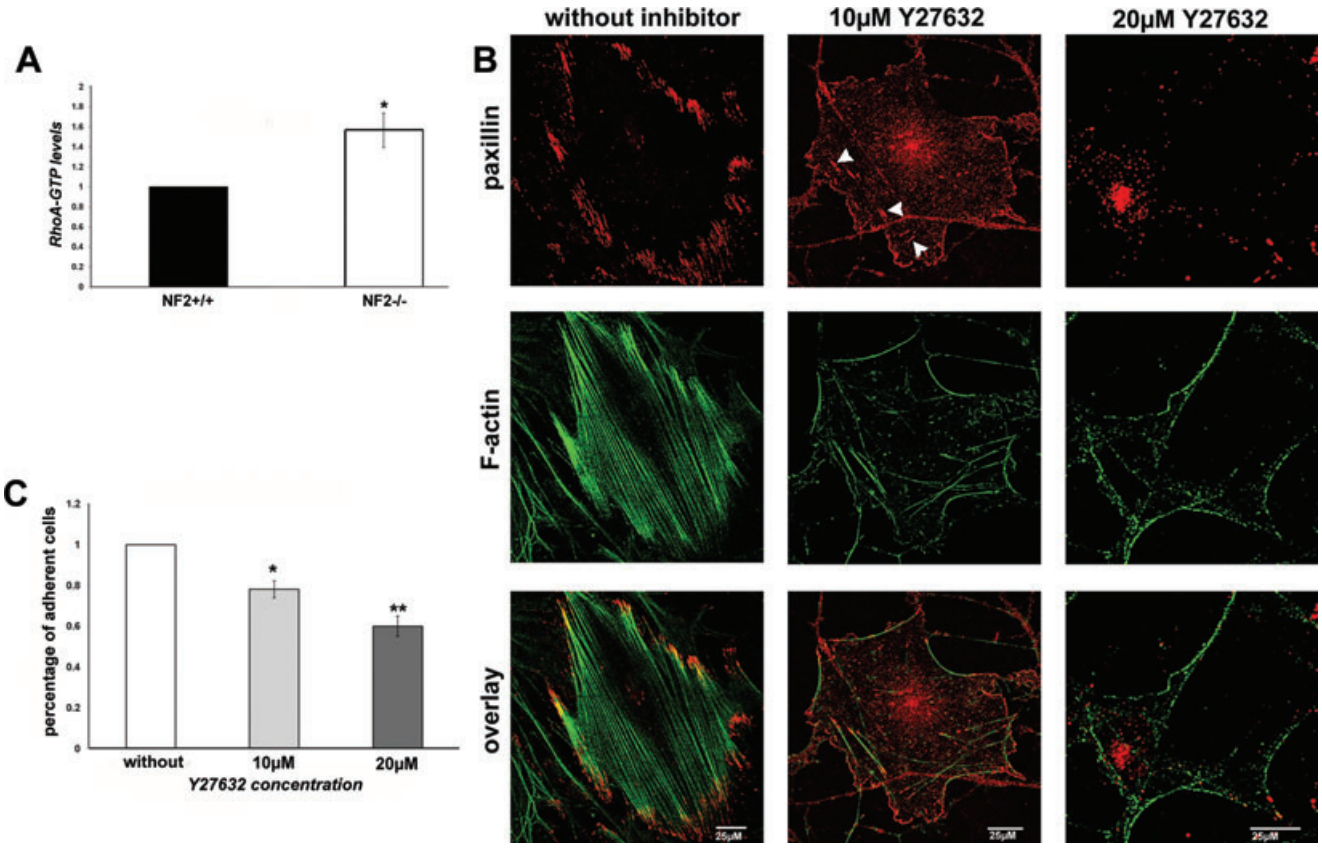

Figure 5. *RhoA activation in human primary Schwann (NF2+/+) and Schwannoma cells (NF2–/–) and RhoA signaling toward focal contacts and adhesion in human primary Schwannoma cells (NF2–/–).* GLISA analysis for RhoA activation shows an increase of RhoA-GTP in human primary Schwannoma cells (NF2–/–) compared with human primary Schwann cells (NF2+/+) (**A**) (*: significant; $P < 0.05$ in student's *t*-test). Human primary Schwannoma cells (NF2–/–) show big focal adhesions and many actin stress fibers (**B**). When RhoA signaling is inhibited with 10 μM of the chemical ROCK inhibitor Y27632 only few big focal adhesions can be detected in human primary Schwannoma cells (NF2–/–) (arrows) and most stress fibers get lost. An intense paxillin staining can be observed around the membrane. Treatment with 20 μM of Y27632 caused a complete loss of focal contacts and stress fibers. Images have been taken on a Zeiss 510meta confocal microscope using a 63* objective. 10 μM of Y27632 caused a decrease in adhesion to around 80% of adhesion without inhibitor (*: significant; $P < 0.05$ in student's *t*-test) and 20 μM to around 60% of adhesion without inhibitor (**: highly significant; $P < 0.01$ in student's *t*-test) (**C**). NF = neurofibromatosis; GFP = green fluorescent protein.

Cdc42-GTP activate PAK that in an inactive state localizes to focal adhesions in a complex with Pix and paxillin. Through the following autophosphorylation, PAK releases from beta-Pix which then can exert its function as a GEF in focal contacts and activate Rac1. The model suits to Schwannoma that show elevated levels of active Cdc42 and integrin activation (11, 46). We, therefore, used the cell permeable inhibitor WR-PAK18 consisting of 18 amino acids of the PAK molecule (25, 26) that binds to the SH3-domain of Pix and prevents Pix-associated Rac1 activation. If Rac1 gets activated through Pix in focal contacts in Schwannoma cells, blocking of Pix should reduce Rac1 activity in our system. If Rac1 activity in turn is relevant for pathological adhesion in Schwannoma, blocking with WR-PAK18 should result in reduced adhesion. 5 μM of WR-PAK18 is the highest possible concentration, where cells stay viable (determined by cell viability assays in human primary Schwann and schwannoma cells; data not shown). 5 μM of WR-PAK18 caused a decrease in Rac1 activation of about 50.57% of Rac1 activation in Schwannoma without inhibitor (Figure 6B) ($P < 0.05$ in student's *t*-test). 5 μM of WR-PAK18 reduced adhesion to 50.20% of the value of Schwannoma cell adhesion without inhibitor (Figure 6C) ($P < 0.01$ in student's *t*-test). Using WR alone did not cause a change in adhesion (data not shown). These results show that at least part of the abnormal Rac1 activation in Schwannoma cells occurs at the levels of focal contacts through the GEF beta-Pix, and that in addition to RhoA, Pix and Rac1 play a crucial role in adhesion in Schwannoma.

DISCUSSION

The previously reported increased adhesion to the extracellular matrix and the activation of integrins (46) prompted us to investigate focal contacts in Schwannoma. We first performed immunocytochemistry using the focal contacts markers paxillin and FAK, to investigate number and size of focal contacts in merlin-deficient human primary Schwannoma and, for direct comparison, in healthy human primary Schwann cells. Both, staining for paxillin and

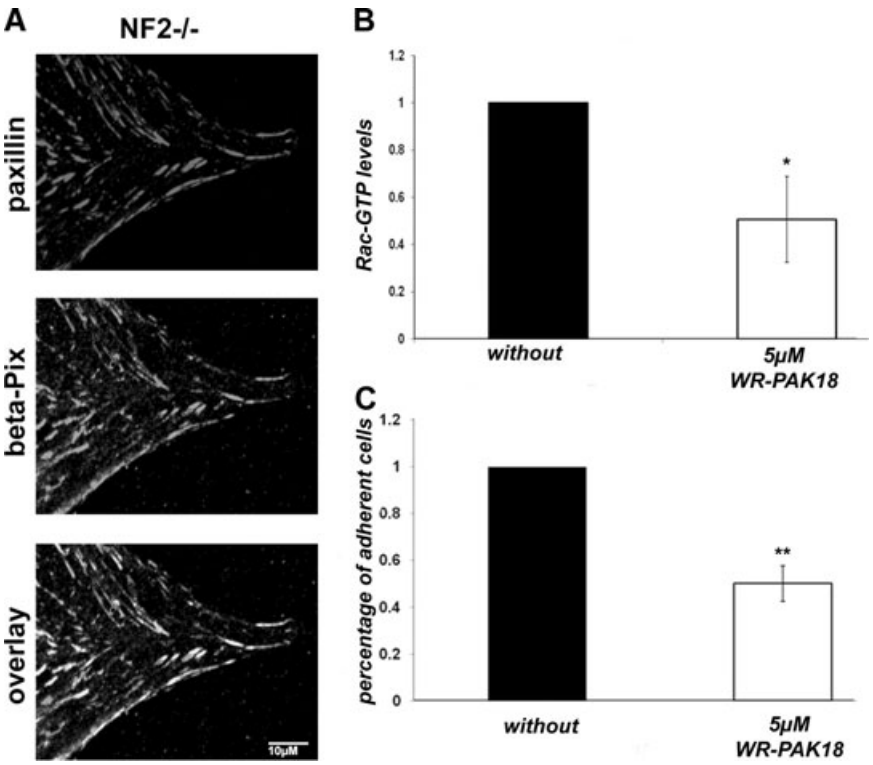

Figure 6. *Regulation of adhesion by Rac-Pix-PAK signaling and the role of focal adhesions in Rac1 activation in human primary Schwannoma cells (NF2–/–).* The Rac1 guanine exchange factor beta-Pix co-localizes with paxillin in focal contacts in human primary Schwannoma cells (NF2–/–) (**A**). Blocking of beta-Pix with the cell permeable inhibitor WR-PAK18 reduces levels of Rac-GTP (measured by GLISA) to 50.57% of Rac-GTP levels without inhibitor (*: significant; $P < 0.05$ in student's *t*-test) in human primary Schwannoma cells (**B**). WR-PAK18 reduces the percentage of adherent human primary Schwannoma cells (NF2–/–) from 100% (without inhibitor) to 50.2% (**: highly significant; $P < 0.01$ in student's *t*-test) (**C**). NF = neurofibromatosis; GFP = green fluorescent protein.

FAK, show more focal contacts in Schwannoma cells than in Schwann cells. As cell spreading is dependent on focal contacts, cell surface is, as expected, larger in human primary Schwannoma cells than in healthy human primary Schwann cells, which have less focal contacts. In addition, focal contacts are larger and localize more distant from the lamellipodia in human primary Schwannoma cells. This is in agreement with previous findings (35) that demonstrate paxillin-stained focal contacts in merlin-deficient Schwannoma cells. Interestingly, a recent study showed that merlin-deficient meningioma cells show numerous focal contacts that are scattered throughout the cell as well (18). The number, size and localization indicate that focal contacts in Schwannoma cells are more mature than their counterparts in Schwann cells. We, therefore, further characterized focal contacts according to their molecular composition. Short living focal complexes interact with the Arp2/3 complex in the lamellipodium (8, 52), whereas mature focal adhesions contain zyxin and localize to the tip of stress fibers. We show that focal contacts in Schwann cells localize to the lamellipodia and staining for paxillin at least partly overlaps with the stain for the Arp2/3 complex. The overlap is not complete as the Arp2/3 complex is mainly involved in actin-branching, and therefore, formation of protrusion and cell motility (41). In line with the Arp2/3 staining, focal contacts in Schwann cells are nearly totally devoid of zyxin and do not co-localize with actin stress fibers. The zyxin staining gives a background staining outside of focal contacts, as it is supposed to be a intracellular signal transducer that can also be found in stress fibers and dynamic cell membrane areas such as the leading edge (1). Taken together, the molecular composition of focal contacts in Schwann cells suggests them being focal complexes that are, according to their association with the Arp2/3 complex, mainly involved in formation of protrusions. In Schwannoma cells on the contrary, the molecular composition indicates that the many focal contacts in Schwannoma cells are mostly stable and mature focal adhesions. Focal adhesions are strong and stable cell-matrix-interaction sites and they fit well to the benign and non-metastatic character of Schwannoma cells that show adhesion to the extracellular matrix and a larger cell surface area. To further investigate if the merlin-deficiency is the main cause for these alterations we reintroduced merlin into human primary Schwannoma cells, using an adenoviral approach. Infection of cells with a GFP control vector alone did not change number, morphology and localization of focal contacts. Human primary Schwannoma cells that re-express merlin, however, show a Schwann cell-like morphology and paxillin stainig can only be found around the membrane in the lamellipodia. Merlin re-expressing Schwannoma cells do not show focal contacts, indicating not only that merlin is involved in the maintenance of focal adhesions, but also that reintroduction of merlin is artificial as it is very difficult to achieve physiological expression levels of the protein. We, therefore, believe that our system of human primary Schwann and Schwannoma cells is the best to study physiological effects of merlin-deficiency. A number of morphology and molecular composition of focal contacts in human primary Schwannoma cells point to a disturbance in the assembly/disassembly of those structures. We, therefore, transfected human primary Schwann and schwannoma cells with either paxillin-GFP or zyxin-GFP. We chose those two constructs as both probes can be used to investigate adhesion turnover (39, 48) and give comparable patterns for the turnover rate in our system. Transfection with these constructs does not alter cell morphology or focal contacts. We determined size and intensity of

focal contacts initially and after 24 minutes. Focal contacts usually have a turnover rate of within a few seconds to a few minutes (51) and we found that 24 minutes are sufficient to see turnover of focal contacts in healthy human primary Schwann cells. We calculated the change in size and intensity separately and then added both values, as they are dependent on each other. A total change of ±20% was taken as negligible and within the accuracy limits of the method. According to the total change three different categories were defined: "equal" for focal contacts with a positive or negative total change of maximal 20%, "appeared and bigger" for focal contacts that do not exist initially or with a positive total change of more than 20%, and "disappeared and smaller" for focal contacts that are not apparent anymore after 24 minutes or have a negative total change of more than 20%. Schwann and Schwannoma cells have very similar levels of focal contacts that appear newly or get bigger, suggesting that the assembly rate of focal contacts is quite similar in both cell types. Schwannoma cells, however, show significantly less focal contacts that get smaller or disappear completely and more focal contacts that stay equal in intensity and size than Schwann cells. These findings imply that Schwannoma cells show less disassembly of focal contacts than Schwann cells. We suggest that the numerous, mature and big focal contacts occur not because of increased assembly but rather because of a disturbed disassembly in human primary Schwannoma cells. To further confirm those findings and because beside changes in size and intensity, movement of focal contacts can be indicative for their turnover; we chose another method to visualize changes in focal contacts: we color-coded images of representative Schwann and Schwannoma cells. In Schwann cells focal contacts found after 24 minutes do neither in shape nor in position resemble the initial focal contacts. Accordingly, nearly no yellow focal contacts can be observed in the overlay images. This confirms our findings from the other method: focal contacts in Schwann cells show ongoing assembly and disassembly. In Schwannoma cells only few of the little focal contacts disassemble (green in the overlay image). Nearly all big focal adhesions are yellow in the overlay images. Taken together, the observation that focal contacts in Schwannoma cells are markedly different from those in Schwann cells, as they occur in high number and are bigger, more mature and show disturbed disassembly, fits to the previously demonstrated increased adhesion and activation of integrins in Schwannoma (46) and suggests that focal contacts play a role in Schwannoma development.

RhoA is known to regulate focal contacts (5). Previously Pelton *et al* (35) showed that RhoA is involved in stress fiber and focal adhesion formation and suspected RhoA to be hyper-activated in Schwannoma cells. By using the GLISA method we could confirm that Schwannoma cells show elevated levels of RhoA activity when compared with Schwann cells. Blocking of the Rho kinase ROCK with the chemical component Y27632 (45), that is supposed to be the best available RhoA inhibitor that has been used in many studies, reduces focal adhesions, stress fibers and adhesion to the extracellular matrix in a dose-dependent manner in human primary Schwannoma cells. These data do not only strengthen the findings of Pelton *et al*, but also show that RhoA signaling occurs through ROCK, that plays a role in myelination (28). Moreover, we found more evidence that the focal adhesions found in Schwannoma cells are the RhoA-regulated mature ones and using our functional readout for adhesion we could finally show that RhoA signaling trough ROCK is involved in the pathological adhesion in Schwannoma cells.

Rac1, another RhoGTPase, which might be involved in focal contacts, is activated in merlin-deficient Schwannoma cells. Pix is a Rac1 GEF that is pivotal for integrin-mediated Rac1 activation (6). Beta-Pix localizes to focal contacts in a complex with PAK1 through binding to paxillin (24, 38). In a recent publication ten Klooster *et al* (42) suggest an interesting model for Rac1 activation in which an integrin-mediated activation of Cdc42 in the leading edge of motile cells leads to the activation of PAK1 which is bound to beta-Pix in focal contacts. The activated PAK1 dissociates from beta-Pix and subsequently Rac1 gets recruited to focal complexes, where it gets activated to induce actin branching and the formation of protrusions. As merlin has been shown to inhibit PAK (15, 22) merlin deficient Schwannoma may be a living example for this model as integrins, Rac1, Cdc42 and PAK are activated in the leading edges (11, 20, 29). We, therefore, tested if the model above can be used to explain Rac1 activation because of merlin loss and link Rac1 activation to the abnormal focal contacts in Schwannomas. Interestingly beta-Pix seems to localize to the numerous and stable focal contacts in human primary Schwannoma cells. We tested if the previously reported increased Rac1 activation can be linked downstream to the focal contact-associated beta-Pix. We used the cell-permeable Rac-PAK inhibitor WR-PAK18 that has been shown to strongly inhibit the growth of NF2-minus mesothelioma cells (26). WR-PAK18 is the proline-rich domain of 18 amino acids of PAK that binds to the SH3 domain of Pix (25). The use of WR-PAK18 in human primary Schwannoma cells markedly reduced the levels of Rac1-GTP, indicating that Rac1 activation at focal contacts is relevant in Schwannoma. Moreover, blocking of the Pix-mediated Rac1 activation reduces adhesion, suggesting that not only RhoA, but also Rac1 plays a role in the pathological adhesion of human primary Schwannoma cells. Merlin inhibits Rac1 activation and directly binds components of focal adhesions, like beta1 integrin, paxillin (10) and FAK (17). Our results here link these data to Rac1 activation that according to our findings occurs at least partly in focal adhesions in Schwannoma cells. Increased adhesion because of numerous and big focal adhesions is, therefore, linked to Rac1 activation that is a characteristic feature of merlin-deficient Schwannoma cells. As the Rac1 pathway activation accounts for the numerous, highly dynamic protrusions and the inability to interact with the axon (11, 29) our data further strengthen the importance of this pathways in Schwannoma development, suggesting the idea that merlin partly exerts its tumor suppressor function at the level of focal contacts and anyhow helps explain the mechanism of the pathological adhesion of Schwannoma cells.

MATERIAL AND METHODS

Preparation of human primary Schwann and Schwannoma cells

Schwann cells were obtained from peripheral nerves from surgical patients not carrying out any predisposition to a peripheral neuropathy. Schwannomas were kindly provided by NF2 patients after informed consent. Diagnosis of NF2 was based on clinical criteria defined by the NIH Consensus Conference on Neurofibromatosis.

Isolation and culturing were carried out as previously described (37). Briefly, cells were cultured in proliferation medium and grown on poly-L-lysine/laminin coated six-well plates (Greiner bio-one, Stonehouse, UK), eight-well permanox chamber slides (Nunc, Wiesbaden, Germany) or glass-bottom dishes (Mattek, Ashland, MA, USA). At least three different Schwannoma have been compared with three different normal nerves in each experiment. Every experiment was carried out between the second and the fourth passage, when proliferation rates are best and the number of fibroblasts is neglible (less than 2%, routinely checked by S-100 staining).

Reagents and expression constructs

Paxillin-GFP and zyxin-GFP were a gift from K. Rottner (Helmholtz Center for Infection Research, Braunschweig, Germany). ROCK inhibitor Y27632 was from Calbiochem (MERCK, Nottingham, UK) and WR-PAK18 conjugated to TAMRA was from NMI peptides (Reutlingen, Germany).

Immunocytochemistry

Schwann and Schwannoma cells were fixed in 4% paraformaldehyd, permablised with 1% TritonX-100, and blocked with 10% normal goat serum. Cells were incubated with anti-paxillin (1:200, upstate Biotechnology, Lake Placid, NY), anti-FAK (1:100 upstate Biotechnology), anit-FAK Tyr397 (FAKY397) (1:100 Chemicon Europe, Hampshire, UK) anti-p34-Arc (1:100 upstate Biotechnology), anti-zyxin (1:100, Sigma-Aldrich, St.Louis, MA, USA) and anti-beta-Pix (1:100, Santa Cruz Biotechnology, Santa Cruz, CA, USA). Appropriate Cy3, or Alexa Fluor 488-labeled secondary antibodies, was used. Alexa Fluor 488-labeled phalloidin was used to visualize filamentous actin (1:100 Molecular Probes, Eugene, OR, USA). Before being cover slipped, cells were mounted with Vecta Shield (Vector Laboratories, Burlingame, CA, USA). As a control, the primary antibody was omitted once in every experiment. Cells were examined with a Zeiss meta510 confocal microscope using a 63× oil objective and the LSM software package (Zeiss, Jena, Germany).

Number and size of focal contacts were analyzed using paxillin stainings of human primary Schwann and Schwannoma cells. Focal contacts were manually counted in 53 Schwann cells from four different donors and in 73 Schwannoma cells from seven different patients. Phase contrast images of 53 Schwann cells and 73 Schwannoma cells have been used to determine cell surface area using the Volocity software (Improvision, Coventry, UK). Size of 144 focal contacts in six different Schwann cells from three different donors and 144 in six different Schwannoma cells from three different patients was determined using the Volocity software (Improvision, Coventry, UK). Mean and error of the mean were calculated with the Excel software and a student's *t*-test was performed to measure significance in differences of number and size between Schwann and Schwannoma cells.

Adenoviral infection of human primary Schwannoma cells

Human primary Schwannoma cells were plated on poly-L-lysine/laminin coated eight-well permanox chamber slides (Nunc, Wiesbaden, Germany) or glass-bottom-dishes (Mattek, Ashland, MA, USA) in proliferating medium. Cells were infected with either control GFP adenovirus or adenovirus co-expressing GFP plus wild-type merlin protein using the protocol previously described (34). Forty-eight hours after addition of adenovirus, cells were used for live cell imaging or fixed for immunocytochemistry.

Focal contacts turnover assay

Human primary Schwann and Schwannoma cells were cultured on poly-L-lysine/laminin coated glass-bottomed culture dishes in proliferation medium for 3 days. They were transfected with paxillin-GFP or zyxin-GFP using Lipofectamine2000 (Invitrogene, Paisley, UK). After 48 h, live cell imaging was performed on a Zeiss meta510 confocal microscope. Using the Volocity software, polygons were manually drawn around focal contacts and size and intensity were determined in the first and the 50th frame (that corresponds to approximately 24 minutes). The values for size and intensity in frame 50 were subtracted from the values in frame 1, giving a negative value when intensity or size gets smaller and a positive value when intensity or size gets bigger. As both, change in intensity and size is indicative for a turnover of the focal contact; we added both values. Three groups were defined: "equal" for focal contacts with a total change of size and intensity under ±20% that we claim is within the limits of the method, "disappeared and smaller" for focal contacts with a negative total change in size and intensity under –20% or that could not be detected in frame 50, "appeared and bigger" for focal contacts that have an increase of size and intensity over 20% or could only be detected in frame 50. In total, 155 focal contacts in nine different cells from four different Schwann cell donors and 219 focal contacts in 12 different cells from six different Schwannoma patients were measured. Mean and standard error of the mean were calculated and student's *t*-test was performed to test significance between Schwann and Schwannoma cells.

As not only change of size and intensity, but also movement is indicative for focal contact turnover, we chose another method in order to visualize adhesion dynamics in Schwann and Schwannoma cells. Focal contacts in frame one were colored green and red in frame 50 using Adobe Photoshop (Adobe, San Jose, CA, USA). When both frames were overlayed, newly appeared focal contacts appear in red, disappeared ones in green and stable ones in yellow.

RhoA and RacGLISA

For measuring RhoA-GTP levels, human primary Schwann and Schwannoma cells were cultured in poly-L-lysine/laminin coated six-well plates until 70% confluent. Cells were serum starved overnight and stimulated with 10% FCS (PAA, Pasching, Austria), 0.5 μM forskolin (Sigma-Aldrich), 10 nM β1-heregulin$_{144–244}$ (Mark Sliwkowski, Genentech, San Francisco, CA, USA), 0.5 mM 3-isobutyl-1-methylxanthin (IBMX, Sigma-Aldrich) and 2.5 μg/ml insulin (Sigma-Aldrich) for 3 minutes. RhoA-GTP was detected using the GLISA Rho activation assay Biochem Kit™ (absorbance-based) from Cytoskeleton (Denver, CO, USA). Briefly, cells were lysed according to the manufacturer's protocol. Protein was estimated, appropriately, diluted in binding buffer and incubated on 96-well plates that contain the RhoA-GTP-binding protein

Rhotekin linked to the bottom of each well. The bound RhoA-GTP is detected with a RhoA-specific primary antibody and a HRP-conjugated secondary antibody. The signal produced by the horseradish peroxidase (HRP) detection reagent and dependent on the amount of RhoA-GTP can be detected by measuring absorbance at 490 nM. Appropriate controls have been carried out (positive control: Rho control protein; negative control: lysis buffer alone). Levels of RhoA-GTP in human primary Schwannoma cells were normalized to RhoA-GTP levels in human primary Schwann cells. Schwann cells from three different donors and Schwannoma cells from three different patients have been used. Mean and standard error of the mean have been calculated with excel and a student's *t*-test has been performed to find out whether the detected difference is significant.

For measuring the effect of the cell permeable inhibitor WR-PAK18 on Rac activation, human primary Schwannoma cells were cultured in poly-L-lysin/laminin coated six-well plates until 70% confluent. Cells were serum starved over night, pre-incubated with 5 µM WR-PAK18 for 30 minutes and stimulated with 10% FCS (PAA), 0.5 µM forskolin (Sigma-Aldrich), 10 nM β1-heregulin$_{144–244}$ (Genentech), 0.5 mM IBMX (Sigma) and 2.5 µg/ml insulin (Sigma-Aldrich) for 3 minutes. Rac1-GTP was detected using the GLISA Rac1 activation assay, Biochem Kit™ (absorbance-based) from cytoskeleton using the afore mentioned procedure. Levels of Rac1-GTP in WR-PAK18 treated human primary Schwannoma cells from three different patients have been normalized to the corresponding untreated cells. Mean and standard error of the mean have been calculated with excel and a student's *t*-test has been performed to find out whether the detected difference is significant.

Adhesion assay

Human primary Schwannoma cells were trypsinized and re-suspended in proliferation medium. Duplicates of 5000 cells per condition have been seeded in poly-L-lysine treated 24-well plates. Cells have been left untreated, treated with 10 µM Y27632, 20 µM Y27632 ROCKII inhibitor or with 5 µM TAMRA-labeled WR-PAK18. After 3-h incubation at 37°C, cells were rinsed twice with phosphate buffered saline to wash away loose cells. Adherent cells were fixed in 4% paraformaldehyde and subsequently counted under an Olympus-phase contrast microscope. Number of adherent Schwannoma cells under 10 µM or 20 µM Y27632 and 5 µM WR-PAK18, have been normalized to number of corresponding untreated Schwannoma cells. Schwannoma cells from three different patients have been analyses. Mean and standard error of the mean have been calculated with excel and a student's *t*-test has been performed to find out whether the detected difference is significant.

ACKNOWLEDGMENTS

This research was supported by the Peninsula College of Medicine and Dentistry, Plymouth, UK.

Control adenovirus expressing GFP and virus expressing GFP plus wild-type NF2 were gifts from Dr Joseph Testa (50).

We thank Dr. David Parkinson for his expertise help with the adenoviral transfection and Natalia Ristic for expert technical assistance.

CONFLICT OF INTEREST STATEMENT

There is no conflict of interest.

REFERENCES

1. Beckerle MC (1997) Zyxin: zinc fingers at sites of cell adhesion. *Bioessays* **11**:949–957.
2. Benninger Y, Thurnherr T, Pereira JA, Krause S, Wu X, Chrostek-Grashoff A *et al* (2007) Essential and distinct roles for cdc42 and rac1 in the regulation of Schwann cell biology during peripheral nervous system development. *J Cell Biol* **6**: 1051–1061.
3. Bershadsky AD, Ballestrem C, Carramusa L, Zilberman Y, Gilquin B, Khochbin S *et al* (2006) Assembly and mechanosensory function of focal adhesions: experiments and models. *Eur J Cell Biol* **3–4**:165–173.
4. Burridge K, Chrzanowska-Wodnicka M (1996) Focal adhesions, contractility, and signaling. *Annu Rev Cell Dev Biol* **12**:463–518.
5. Burridge K, Wennerberg K (2004) Rho and Rac take center stage. *Cell* **2**:167–179.
6. del Pozo MA, Price LS, Alderson NB, Ren XD, Schwartz MA (2000) Adhesion to the extracellular matrix regulates the coupling of the small GTPase Rac to its effector PAK. *EMBO J* **9**:2008–2014.
7. del Pozo MA, Kiosses WB, Alderson NB, Meller N, Hahn KM, Schwartz MA (2002) Integrins regulate GTP-Rac localized effector interactions through dissociation of Rho-GDI. *Nat Cell Biol* **3**:232–239.
8. DeMali KA, Burridge K (2003) Coupling membrane protrusion and cell adhesion. *J Cell Sci* **116**(Pt 12):2389–2397.
9. Dickersin GR (1987) The electron microscopic spectrum of nerve sheath tumors. *Ultrastruct Pathol* **2–3**:103–146.
10. Fernandez-Valle C, Tang Y, Ricard J, Rodenas-Ruano A, Taylor A, Hackler E *et al* (2002) Paxillin binds schwannomin and regulates its density-dependent localization and effect on cell morphology. *Nat Genet* **4**:354–362.
11. Flaiz C, Kaempchen K, Matthies C, Hanemann CO (2007) Actin-rich protrusions and nonlocalized GTPase activation in merlin-deficient Schwannomas. *J Neuropathol Exp Neurol* **7**:608–616.
12. Flaiz C, Utermark T, Parkinson DB, Poetsch A, Hanemann CO (2008) Impaired intercellular adhesion and immature adherens junctions in merlin-deficient human primary schwannoma cells. *Glia* **56**:506–515.
13. Hall A (1994) Small GTP-binding proteins and the regulation of the actin cytoskeleton. *Annu Rev Cell Biol* **10**:31–54.
14. Hanemann CO, Evans DG (2006) News on the genetics, epidemiology medical care and translational research of Schwannomas. *J Neurol* **12**:1533–1541.
15. Hirokawa Y, Tikoo A, Huynh J, Utermark T, Hanemann CO, Giovannini M *et al* (2004) A clue to the therapy of neurofibromatosis type 2: NF2/merlin is a PAK1 inhibitor. *Cancer J* **1**:20–26.
16. Hotchin NA, Hall A (1995) The assembly of integrin adhesion complexes requires both extracellular matrix and intracellular rho/rac GTPases. *J Cell Biol* **6**:1857–1865.
17. James MF, Beauchamp RL, Manchanda N, Kazlauskas A, Ramesh V (2004) A NHERF binding site links the betaPDGFR to the cytoskeleton and regulates cell spreading and migration. *J Cell Sci Pt* **14**:2951–2961.
18. James MF, Lelke JM, MacCollin M, Plotkin SR, Stemmer-Rachamimov AO, Ramesh V *et al* (2008) Modeling NF2 with human arachnoidal and meningioma cell culture systems: NF2 silencing reflects the benign character of tumor growth. *Neurobiol Dis* **29**:278–292.

19. Jessen KR, Mirsky R (2005) The origin and development of glial cells in peripheral nerves. *Nat Rev Neurosci* **9**:671–682.
20. Kaempchen K, Mielke K, Utermark T, Langmesser S, Hanemann CO (2003) Upregulation of the Rac1/JNK signaling pathway in primary human Schwannoma cells. *Hum Mol Genet* **11**:1211–1221.
21. Kaverina I, Krylyshkina O, Small JV (2002) Regulation of substrate adhesion dynamics during cell motility. *Int J Biochem Cell Biol* **7**:746–761.
22. Kissil JL, Wilker EW, Johnson KC, Eckman MS, Yaffe MB, Jacks T (2003) Merlin, the product of the Nf2 tumor suppressor gene, is an inhibitor of the p21-activated kinase, Pak1. *Mol Cell* **4**:841–849.
23. Lallemand D, Curto M, Saotome I, Giovannini M, McClatchey AI (2003) NF2 deficiency promotes tumorigenesis and metastasis by destabilizing adherens junctions. *Genes Dev* **17**:1090–1100.
24. Manser E, Loo TH, Koh CG, Zhao ZS, Chen XQ, Tan L *et al* (1998) PAK kinases are directly coupled to the PIX family of nucleotide exchange factors. *Mol Cell* **2**:183–192.
25. Maruta H, He H, Tikoo A, Nur-e-Kamal M (1999) Cytoskeletal tumor suppressors that block oncogenic RAS signaling. *Ann N Y Acad Sci* **886**:48–57.
26. Maruta H, Nheu TV, He H, Hirokawa Y (2003) Rho family-associated kinases PAK1 and rock. *Prog Cell Cycle Res* **5**:203–210.
27. McClatchey AI, Saotome I, Mercer K, Crowley D, Gusella JF, Bronson RT *et al* (1998) Mice heterozygous for a mutation at the Nf2 tumor suppressor locus develop a range of highly metastatic tumors. *Gene Dev* **8**:1121–1133.
28. Melendez-Vasquez CV, Einheber S, Salzer JL (2004) Rho kinase regulates schwann cell myelination and formation of associated axonal domains. *J Neurosci* **16**:3953–3963.
29. Nakai Y, Zheng Y, MacCollin M, Ratner N (2006) Temporal control of Rac in Schwann cell-axon interaction is disrupted in NF2-mutant Schwannoma cells. *J Neurosci* **13**:3390–3395.
30. Nobes CD, Hall A (1995) Rho, rac, and cdc42 GTPases regulate the assembly of multimolecular focal complexes associated with actin stress fibers, lamellipodia, and filopodia. *Cell* **1**:53–62.
31. Nodari A, Zambroni D, Quattrini A, Court FA, D'Urso A, Recchia A *et al* (2007) Beta1 integrin activates Rac1 in Schwann cells to generate radial lamellae during axonal sorting and myelination. *J Cell Biol* **6**:1063–1075.
32. Obremski VJ, Hall AM, Fernandez-Valle C (1998) Merlin, the neurofibromatosis type 2 gene product, and beta1 integrin associate in isolated and differentiating Schwann cells. *J Neurobiol* **4**:487–501.
33. Okada T, You L, Giancotti FG (2007) Shedding light on Merlin's wizardry. *Trends Cell Biol* **5**:222–229.
34. Parkinson DB, Bhaskaran A, Droggiti A, Dickinson S, D'Antonio M, Mirsky R, Jessen KR (2004) Krox-20 inhibits Jun-NH2-terminal kinase/c-Jun to control Schwann cell proliferation and death. *J Cell Biol.* **164**(3):385–394.
35. Pelton PD, Sherman LS, Rizvi TA, Marchionni MA, Wood P, Friedman RA *et al* (1998) Ruffling membrane, stress fiber, cell spreading and proliferation abnormalities in human Schwannoma cells. *Oncogene* **17**:2195–2209.
36. Ren XD, Kiosses WB, Schwartz MA (1999) Regulation of the small GTP-binding protein rho by cell adhesion and the cytoskeleton. *EMBO J* **3**:578–585.
37. Rosenbaum C, Kluwe L, Mautner VF, Friedrich RE, Mueller HW, Hanemann CO (1998) Isolation and characterization of Schwann cells from neurofibromatosis type 2 patients. *Neurobiol Dis* **1**:55–64.
38. Rosenberger G, Kutsche, K (2006) AlphaPIX and betaPIX and their role in focal adhesion formation. *Eur J Cell Biol* **3–4**:265–274.
39. Rottner K, Krause M, Gimona M, Small JV, Wehland J (2001) Zyxin is not colocalized with vasodilator-stimulated phosphoprotein (VASP) at lamellipodial tips and exhibits different dynamics to vinculin, paxillin, and VASP in focal adhesions. *Mol Biol Cell* **10**:3103–3113.
40. Sherman L, Xu HM, Geist RT, Saporito-Irwin S, Howells N, Ponta H *et al* (1997) Interdomain binding mediates tumor growth suppression by the NF2 gene product. *Oncogene* **20**:2505–2509.
41. Svitkina TM, Borisy, GG (1999) Arp2/3 complex and actin depolymerizing factor/cofilin in dendritic organization and treadmilling of actin filament array in lamellipodia. *J Cell Biol* **5**:1009–1026.
42. ten Klooster JP, Jaffer ZM, Chernoff J, Hordijk PL (2006) Targeting and activation of Rac1 are mediated by the exchange factor beta-Pix. *J Cell Biol* **5**:759–769.
43. Thurnherr T, Benninger Y, Wu X, Chrostek A, Krause SM, Nave KA *et al* (2006) Cdc42 and Rac1 signaling are both required for and act synergistically in the correct formation of myelin sheaths in the CNS. *J Neurosci* **40**:10110–10119.
44. Tikoo A, Varga M, Ramesh V, Gusella J, Maruta H (1994) An anti-Ras function of neurofibromatosis type 2 gene product (NF2/Merlin). *J Biol Chem* **38**:23387–23390.
45. Uehata M, Ishizaki T, Satoh H, Ono T, Kawahara T, Morishita T *et al* (1997) Calcium sensitization of smooth muscle mediated by a Rho-associated protein kinase in hypertension. *Nature* **6654**:990–994.
46. Utermark T, Kaempchen K, Hanemann CO (2003) Pathological adhesion of primary human Schwannoma cells is dependent on altered expression of integrins. *Brain Pathol* **3**:352–363.
47. Utermark T, Schubert SJ, Hanemann CO (2005) Rearrangements of the intermediate filament GFAP in primary human Schwannoma cells. *Neurobiol Dis* **1**–2:1–9.
48. Webb DJ, Donais K, Whitmore LA, Thomas SM, Turner CE, Parsons JT *et al* (2004) FAK-Src signalling through paxillin, ERK and MLCK regulates adhesion disassembly. *Nat Cell Biol* **2**:154–161.
49. Xiao GH, Beeser A, Chernoff J, Testa JR (2002) p21-activated Kinase Links Rac/Cdc42 Signaling to Merlin. *J Biol Chem* **2**:883–886.
50. Xiao G, Gallagher R, Shetler J, Skele K, Altomare D, Pestell R, Jhanwar S, Testa J (2005) The NF2 tumor suppressor gene product, merlin, inhibits cell proliferation and cell cycle progression by repressing cyclin D1 expression. *Mol Cell Biol* **25**:2384–2394.
51. Zaidel-Bar R, Ballestrem C, Kam Z, Geiger B (2003) Early molecular events in the assembly of matrix adhesions at the leading edge of migrating cells. *J Cell Sci* **116**(Pt 22):4605–4613.
52. Zaidel-Bar R, Cohen M, Addadi L, Geiger B (2004) Hierarchical assembly of cell-matrix adhesion complexes. *Biochem Soc Trans* **32**(Pt 3):416–420.
53. Zaidel-Bar R, Itzkovitz S, Ma'ayan A, Iyengar R, Geiger B (2007) Functional atlas of the integrin adhesome. *Nat Cell Biol* **8**:858–867.
54. Zhao ZS, Manser E (2005) PAK and other Rho-associated kinases—effectors with surprisingly diverse mechanisms of regulation. *Biochem J* **386**(Pt 2):201–214.